Electronic Supplementary Material (ESI) for Dalton Transactions.

Supporting Information

Mg-Porphyrin complex doped divinylbenzene based porous organic polymers (POPs) as highly efficient heterogeneous catalysts for the conversion of CO_2 to cyclic carbonates

Wenlong Wang,*[a] Cunyao Li,[b] Jutao Jin,[a] Li Yan,[b] Yunjie Ding*[b]

[a] School of Environment and Civil Engineering, Dongguan University of Technology, Dongguan 523808, China

[b] Dalian National Laboratory for Clean Energy, Dalian Institute of Chemical Physics, Chinese Academy of Sciences, Dalian, 116023, China.

Email: wangwl@dgut.edu.cn, dyj@dicp.ac.cn.

Contents

General information

Carbon dioxide is commercially available with 99.99% purity. All the solvents were purchased with analytically pure without further purification, and epoxides were also purchased with high purity (> 98%).

NMR data were obtained on a Bruker AV-400 MHz spectrometer. TGA curves were measured on a STA449F3 analyzer. Inductively coupled plasma spectroscopy (ICP) was tested on a PerkinElmer apparatus Optima 7300 DV. The CO_2 adsorption isotherms of POPs catalysts at 273 K were carried out on IGA-100A Hiden Analytical.

^{1}H NMR copies of known products

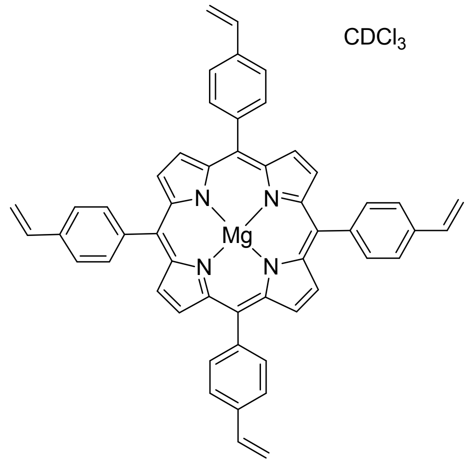
Mg
N
CDCl3

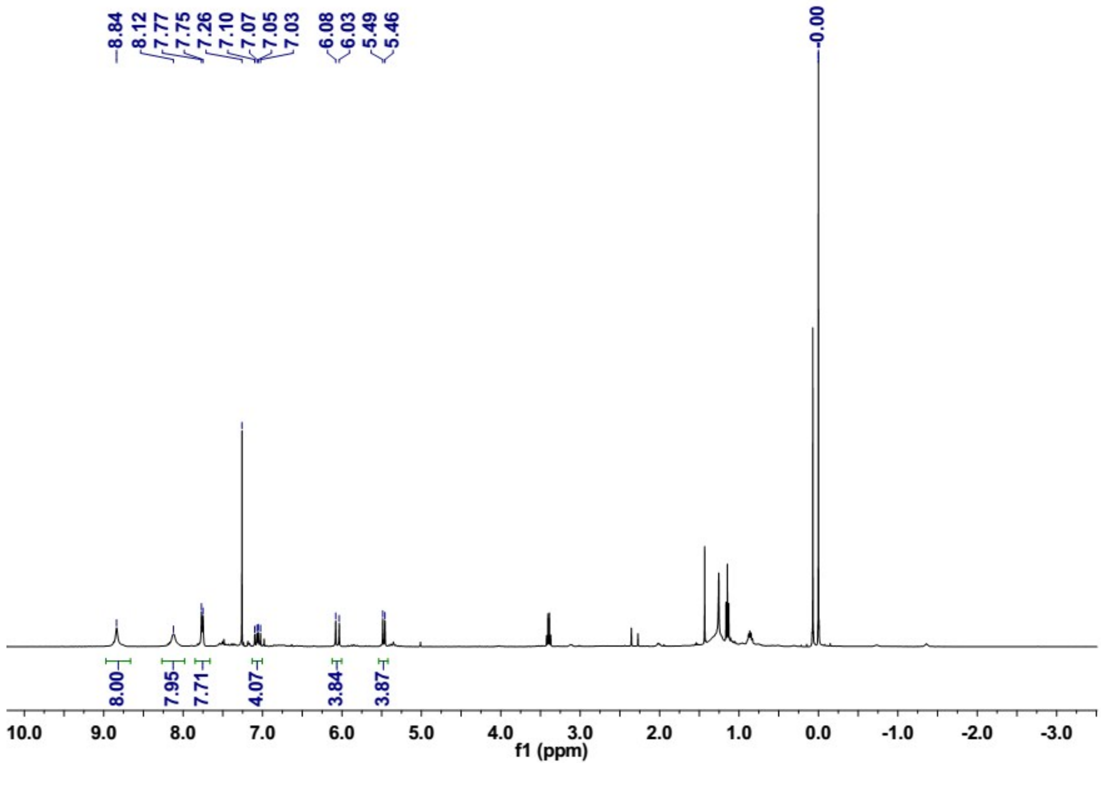
8.84
8.12
7.77
7.75
7.26
7.10
7.07
7.05
7.03
6.08
6.03
5.49
5.46
-0.00
8.00
7.95
7.71
4.07
3.84
3.87
10.0 9.0 8.0 7.0 6.0 5.0 4.0 3.0 2.0 1.0 0.0 -1.0 -2.0 -3.0
f1 (ppm)

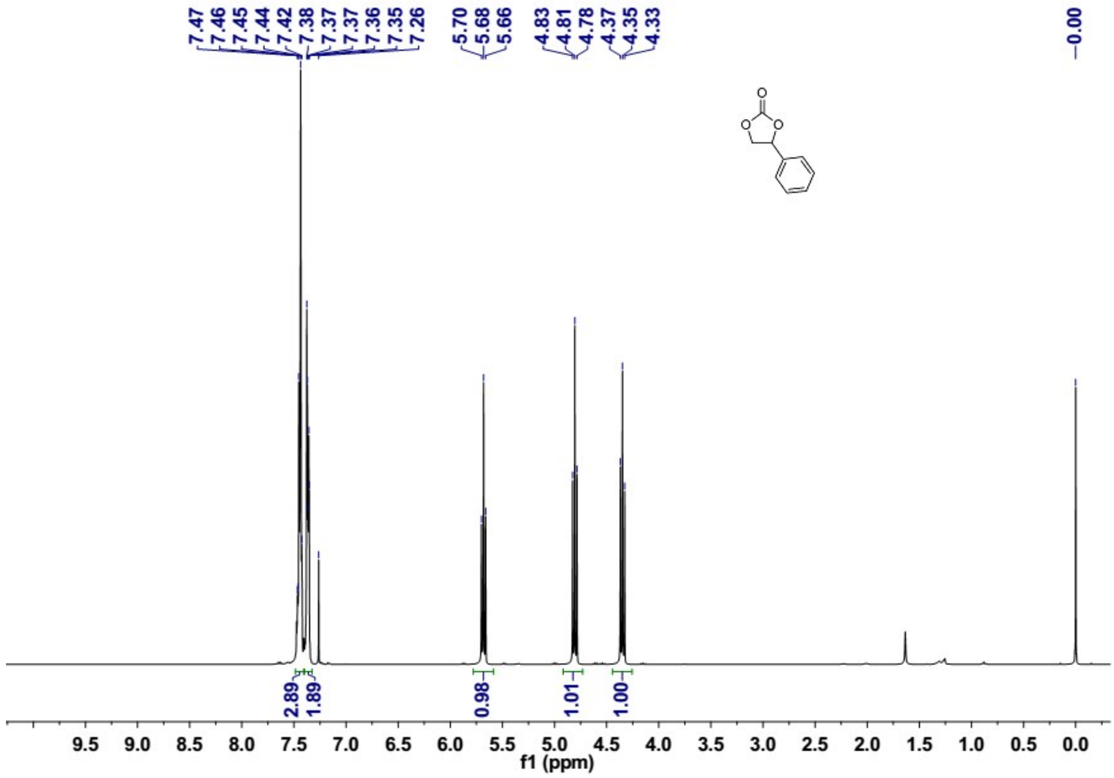
7.47 7.46 7.45 7.44 7.42 7.38 7.37 7.37 7.36 7.35 7.26
5.70 5.68 5.66
4.83 4.81 4.78
4.37 4.35 4.33
0.00
2.89 1.89 0.98 1.01 1.00
f1 (ppm)

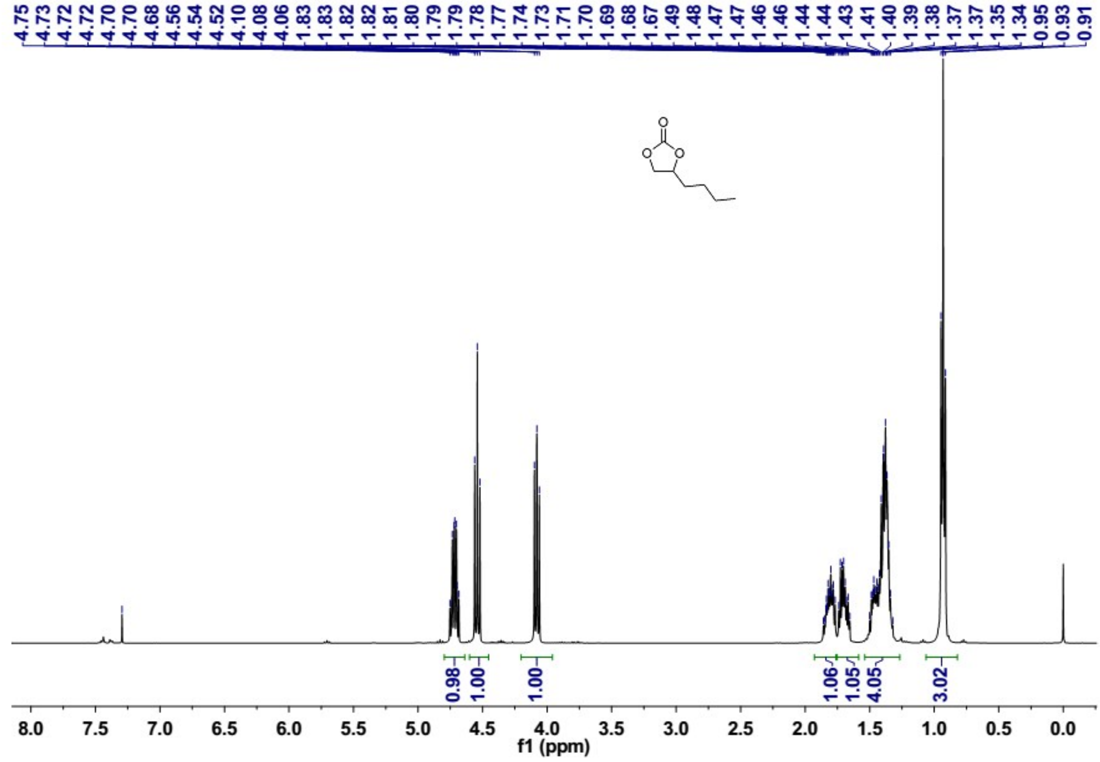
4.75 4.73 4.72 4.72 4.70 4.70 4.68 4.56 4.54 4.52 4.10 4.08 4.06 1.83 1.83 1.82 1.82 1.81 1.80 1.79 1.79 1.78 1.77 1.74 1.73 1.71 1.70 1.69 1.68 1.67 1.49 1.48 1.47 1.47 1.46 1.46 1.44 1.44 1.43 1.41 1.40 1.39 1.38 1.37 1.37 1.35 1.34 0.95 0.93 0.91
0.98 1.00 1.00 1.06 1.05 4.05 3.02
f1 (ppm)

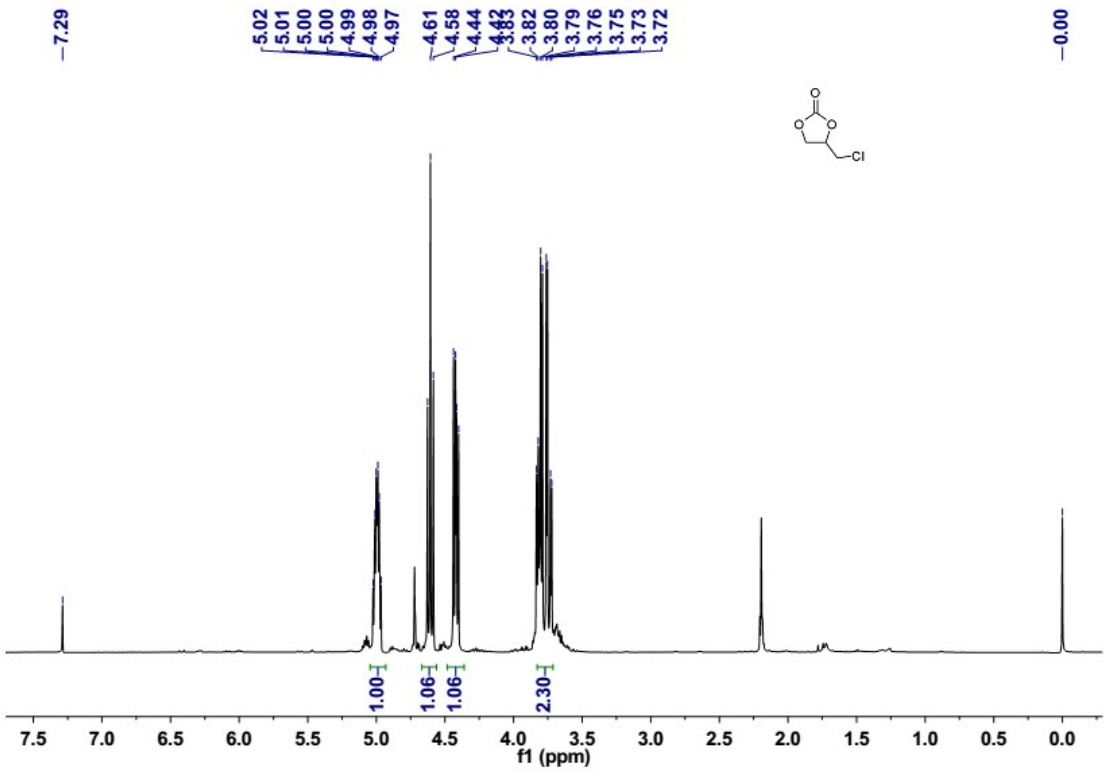

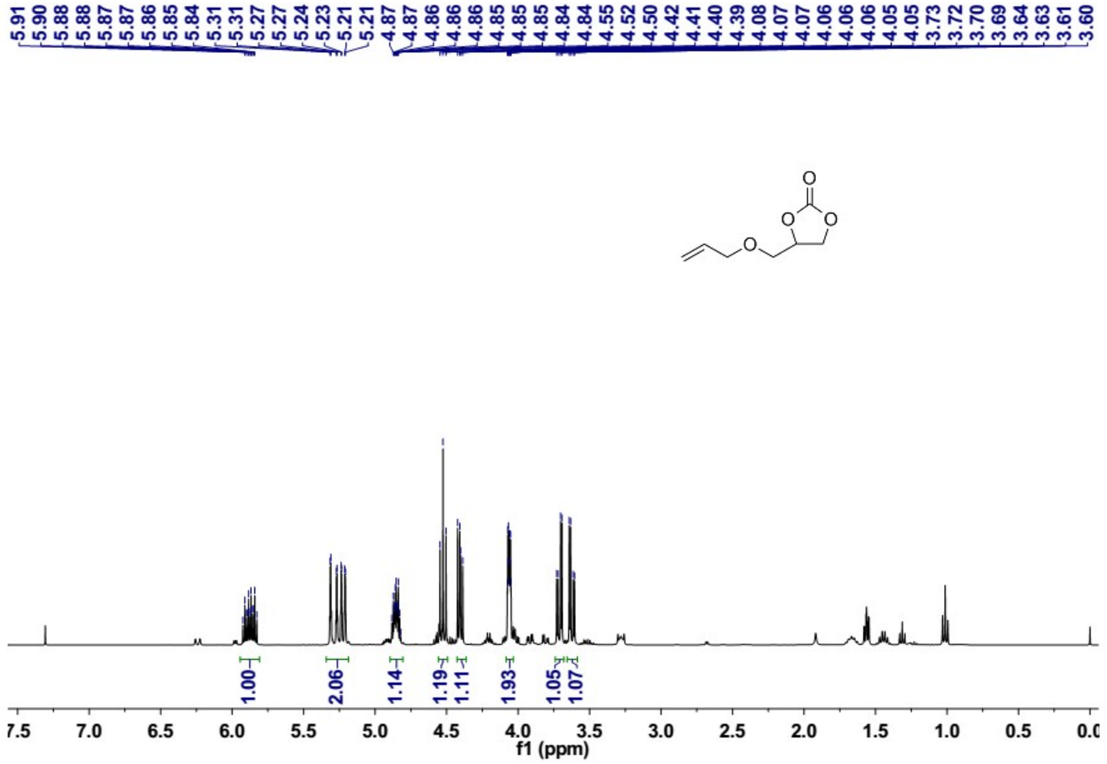

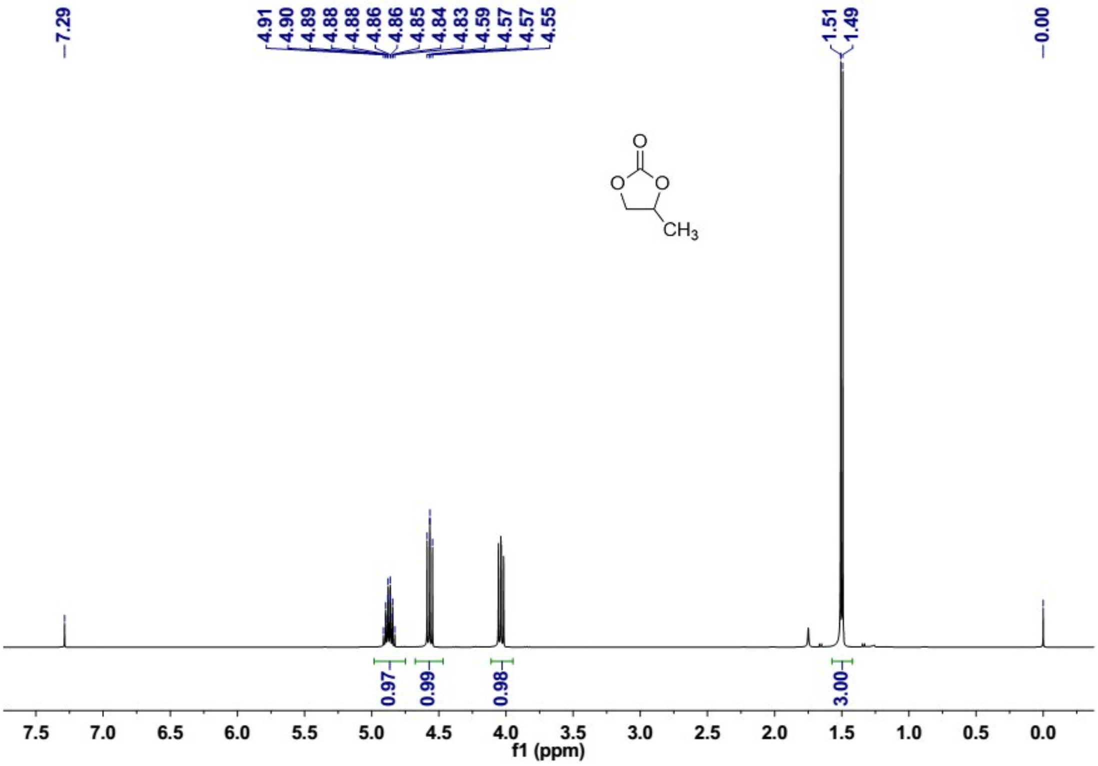

ICP data of Mg-Por\DVB@POPs

Table S1 ICP data of Mg-Por\DVB@POPs with different Mg content.

Sample	Theoretical Mg content (wt %)	Measured Mg content (wt %)
Mg-Por\DVB(1:20)@POPs	0.73	0.70
Mg-Por\DVB(1:40)@POPs	0.41	0.38
Mg-Por\DVB(1:60)@POPs	0.28	0.29
Mg-Por\DVB(1:80)@POPs	0.22	0.20
Mg-Por\DVB(1:100)@POPs	0.18	0.19

Thermal gravimetric analysis (TGA)

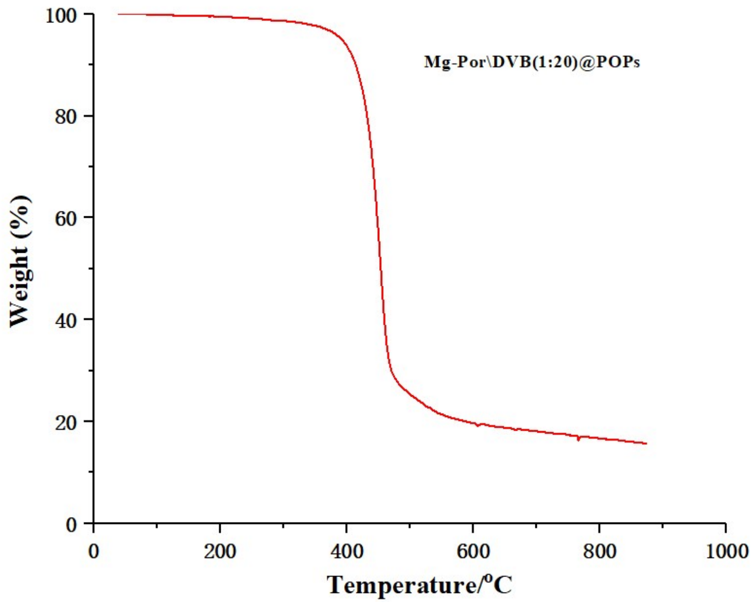

Fig. S1. TGA analysis of Mg-Por\DVB(1:20)POPs

CO_2 adsorption analysis

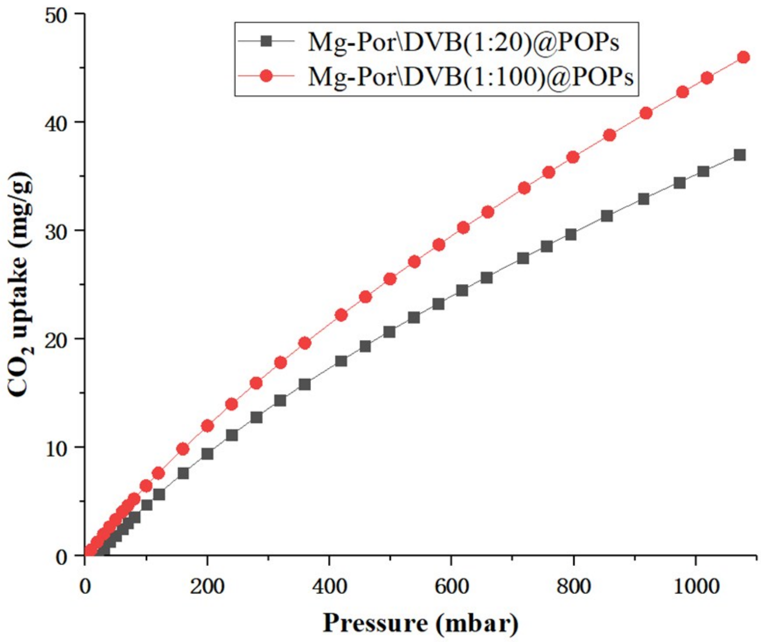

Fig. S2. CO_2 adsorption analysis of Mg-Por\DVB(1:20)@POPs and Mg-Por\DVB(1:100)@POPs

Photograph of solid situation of Mg-Por\DVB(1:20)@POPs

Fig. S3. Photograph of solid situation of Mg-Por\DVB(1:20)@POPs

Representative GC chromatography

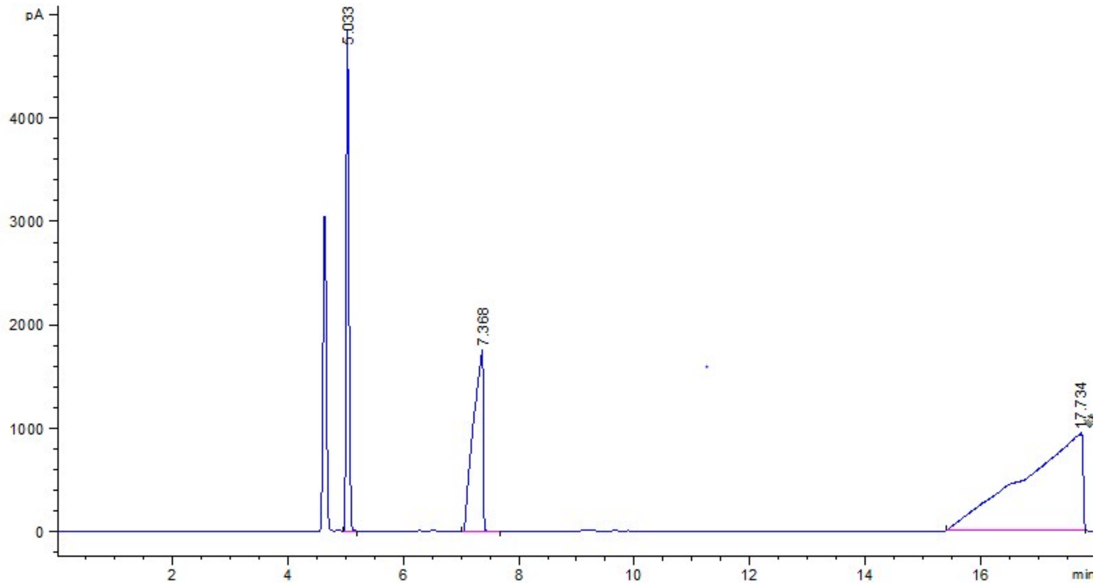

Fig. S4. Representative GC chromatography

Table S2 Detailed information of the representative GC chromatography

Retention time [min]	Peak area [pA*s]	Content [ng/μl]	Substance
5.033	1.64582e4	2.96	Propylene oxide
7.368	2.04866e4	2.10	n-Butyl alcohol (internal standard)
17.734	6.56175e4	13.26	Cyclic carbonate

N_2 adsorption and desorption analysis

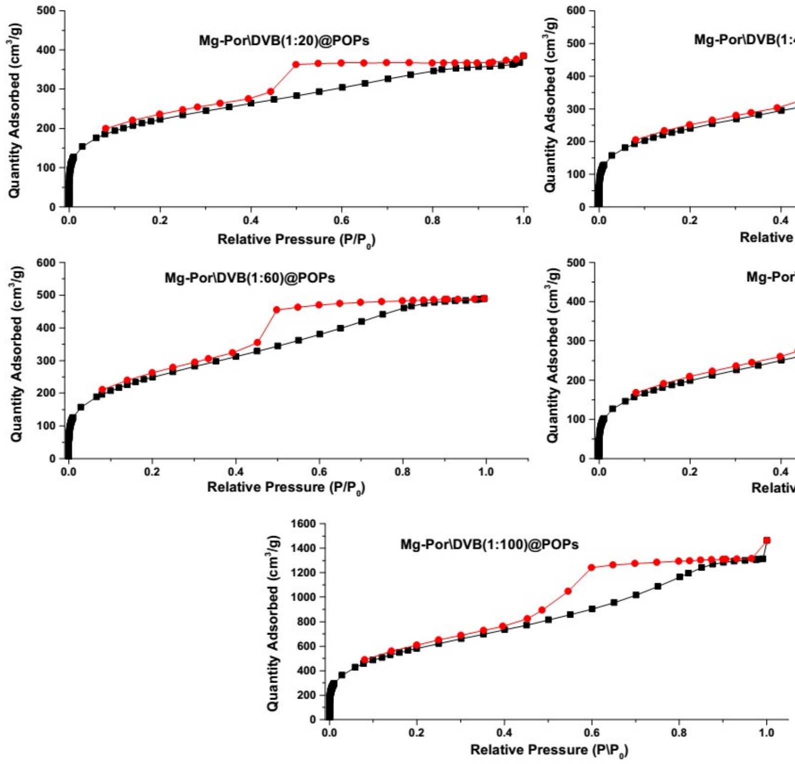

Fig. S5. N_2 sorption isotherms measured at 77 K.

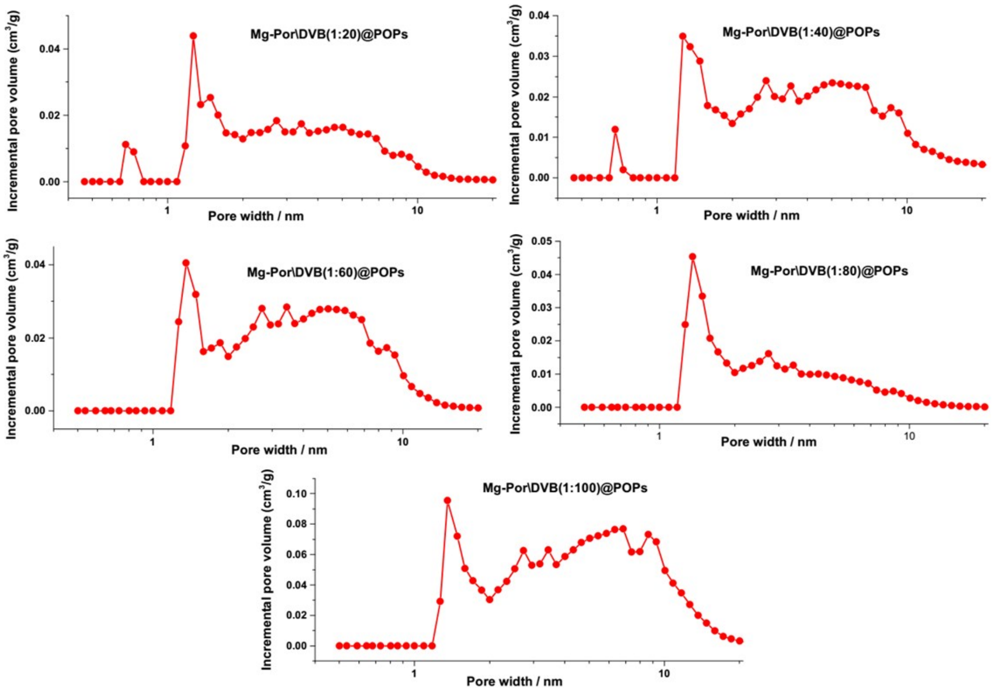

Fig. S6. Pore-size distribution curve of five Mg-Por\DVB@POPs samples calculated by NLDFT method.

SEM&TEM characterization

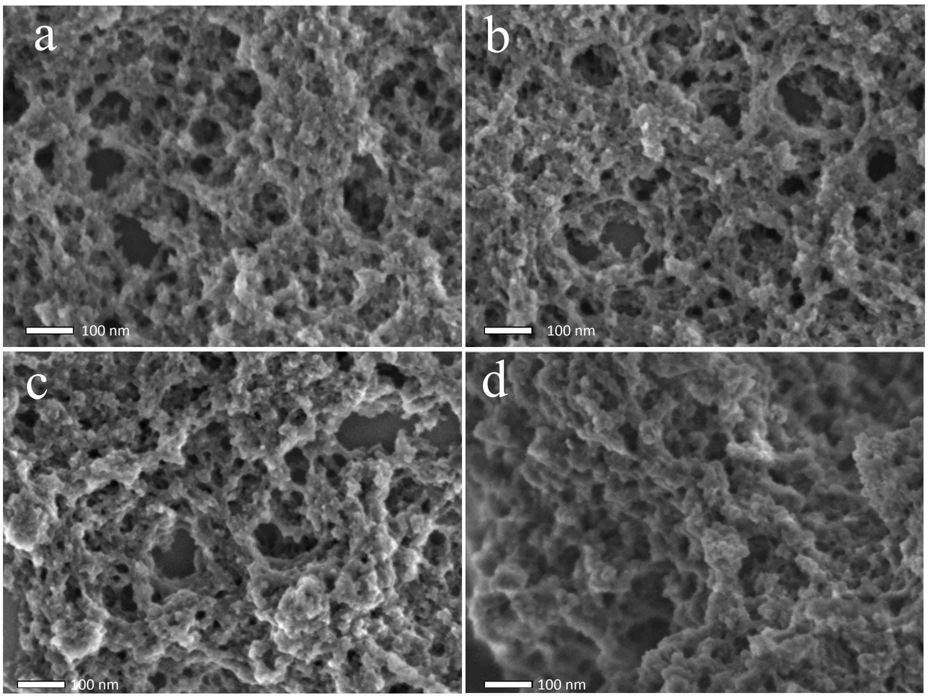

Fig. S7. Representative SEM images of the other four Mg-Por\DVB@POPs samples. a). Mg-Por\DVB(1:40)@POPs; b). Mg-Por\DVB(1:60)@POPs; c). Mg-Por\DVB(1:80)@POPs; d). Mg-Por\DVB(1:100)@POPs.

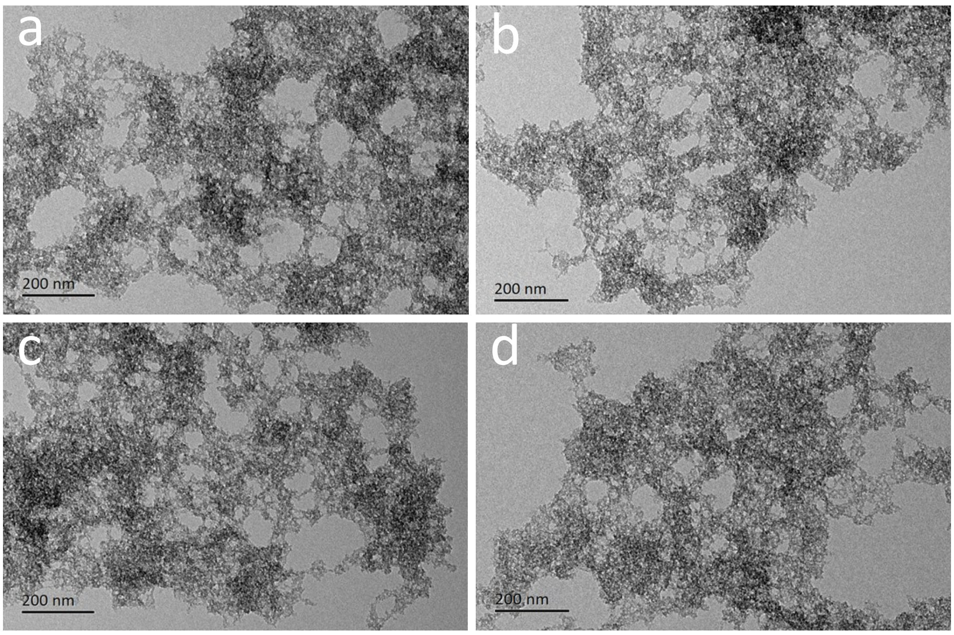

Fig. S8. Representative TEM images of the other four Mg-Por\DVB@POPs samples. a). Mg-Por\DVB(1:40)@POPs; b). Mg-Por\DVB(1:60)@POPs; c). Mg-Por\DVB(1:80)@POPs; d). Mg-Por\DVB(1:100)@POPs.

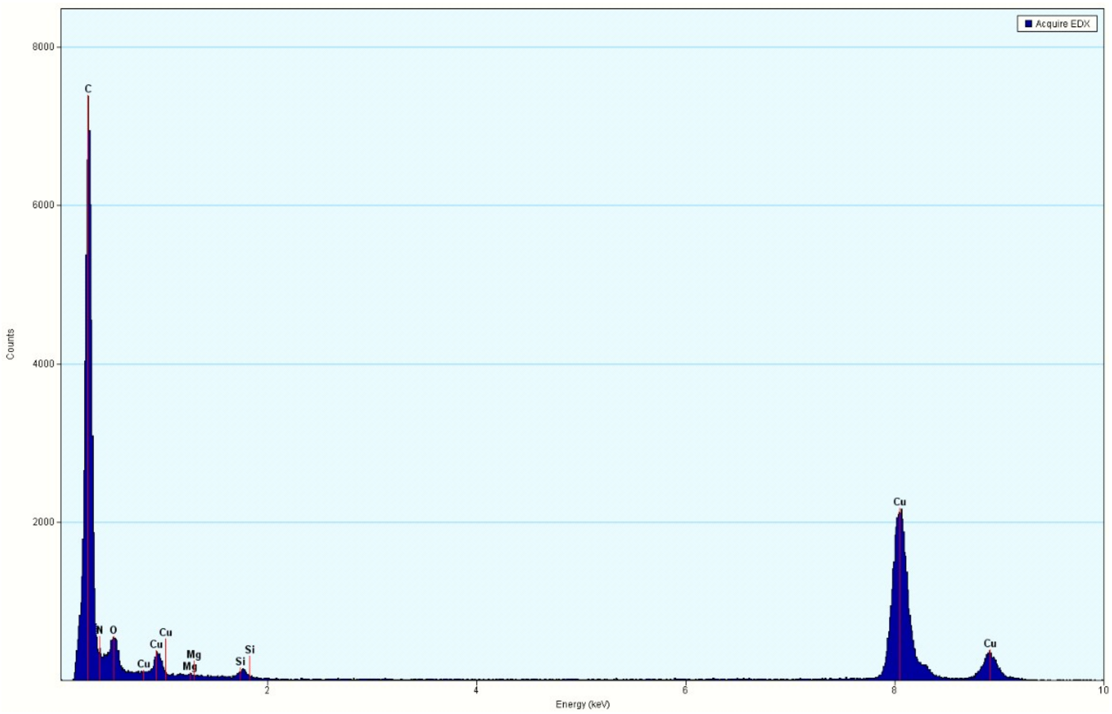

Fig. S9. TEM-EDS Characterization of Mg-Por\DVB(1:20)@POPs

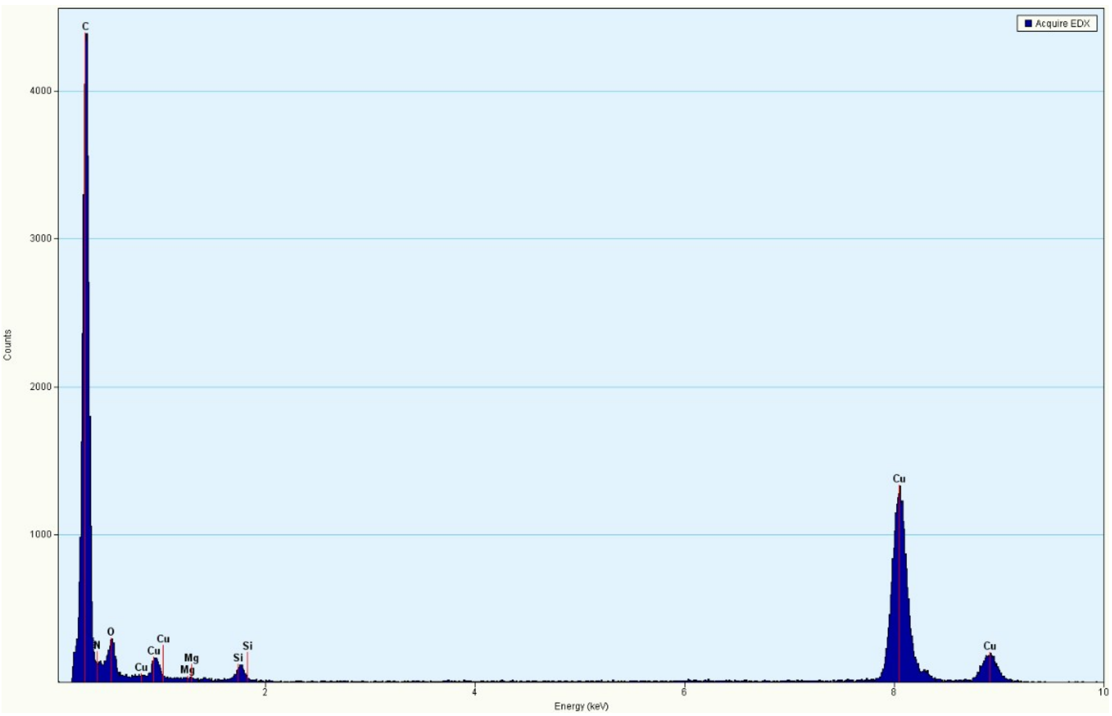

Fig. S10. TEM-EDS Characterization of Mg-Por\DVB(1:40)@POPs

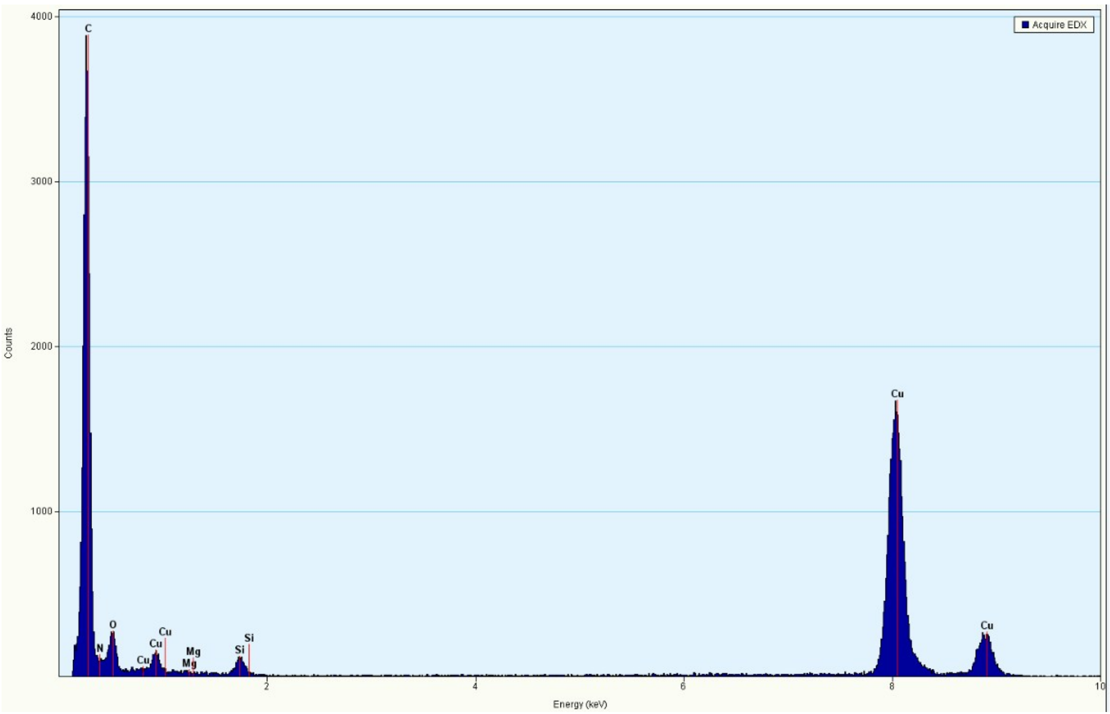

Fig. S11. TEM-EDS Characterization of Mg-Por\DVB(1:60)@POPs

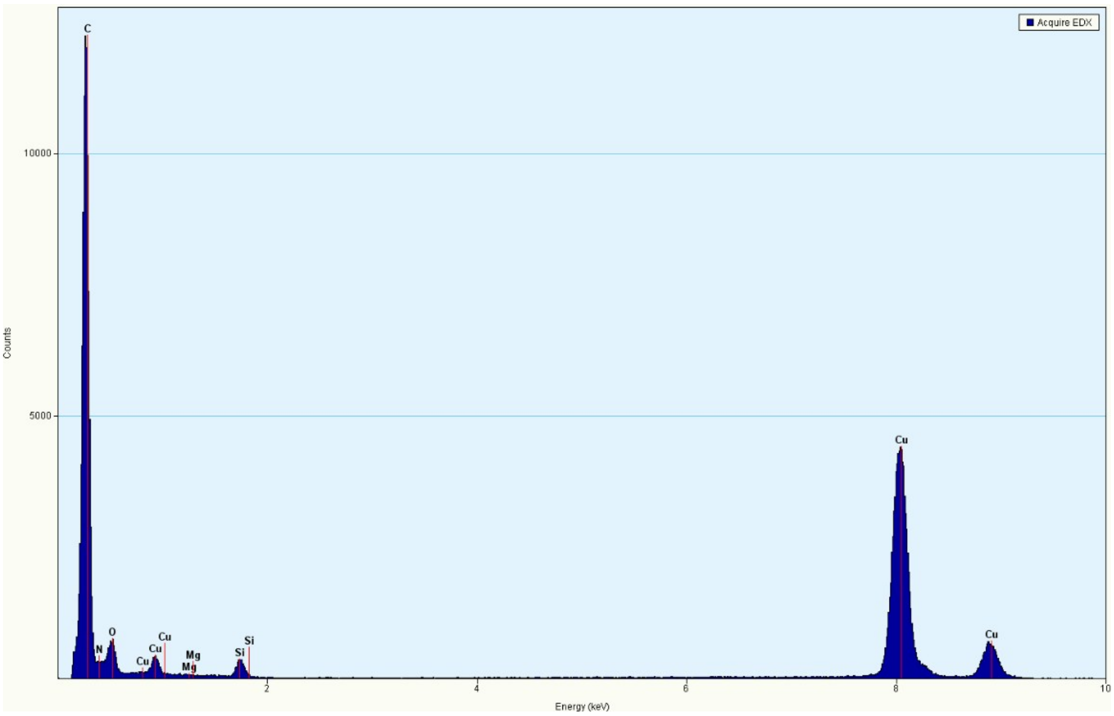

Fig. S12. TEM-EDS Characterization of Mg-Por\DVB(1:80)@POPs

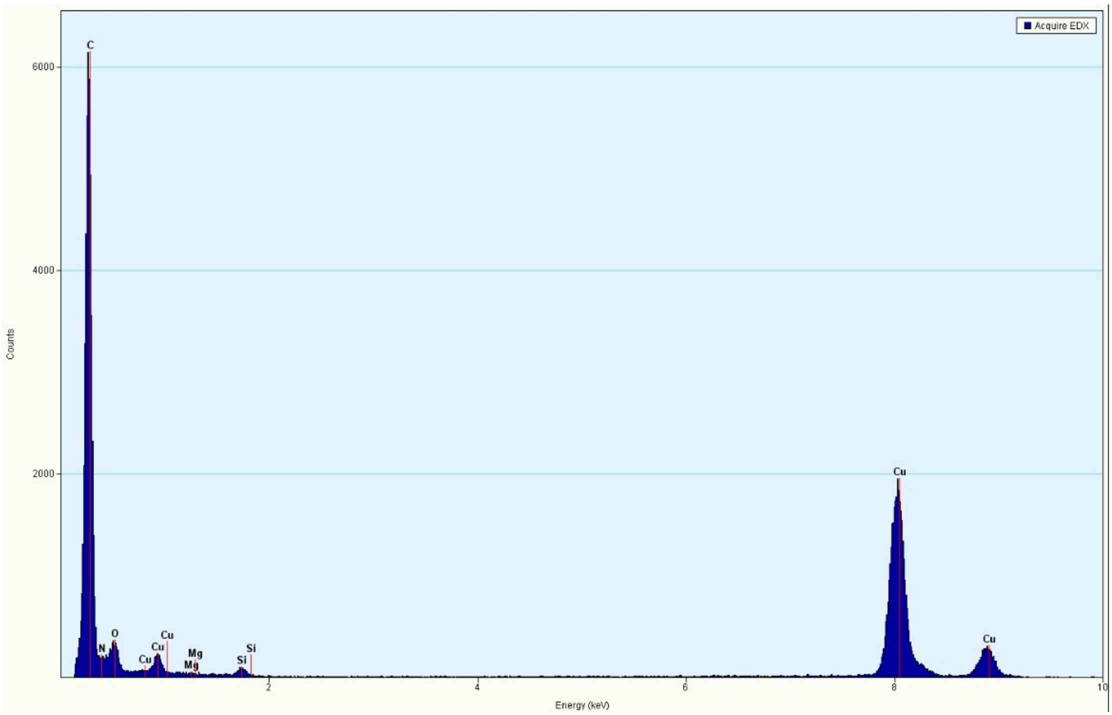

Fig. S13. TEM-EDS Characterization of Mg-Por\DVB(1:100)@POPs

Solid-state ^{13}C NMR spectra

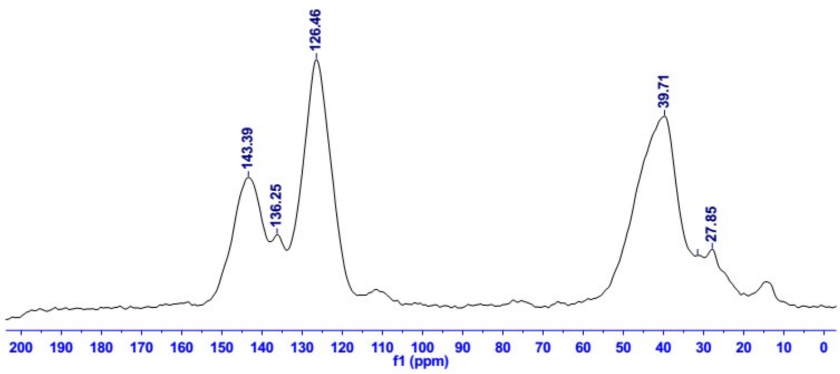

Fig. S14. Solid-state spectrum of Mg-Por\DVB(1:40)@POPs

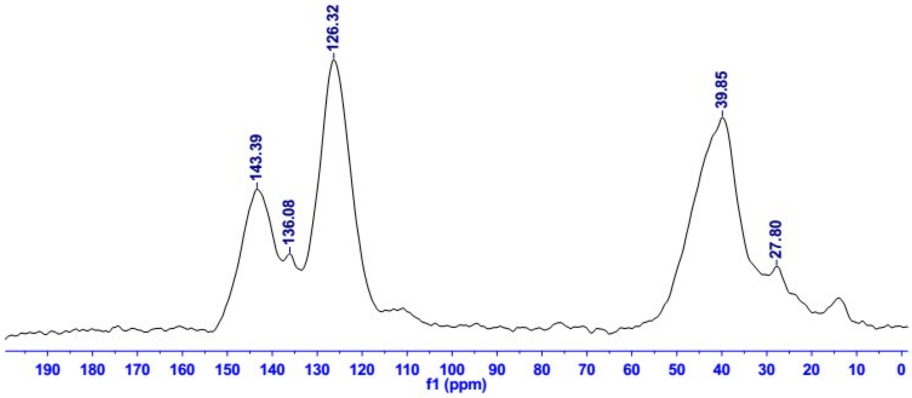

Fig. S15. Solid-state spectrum of Mg-Por\DVB(1:60)@POPs

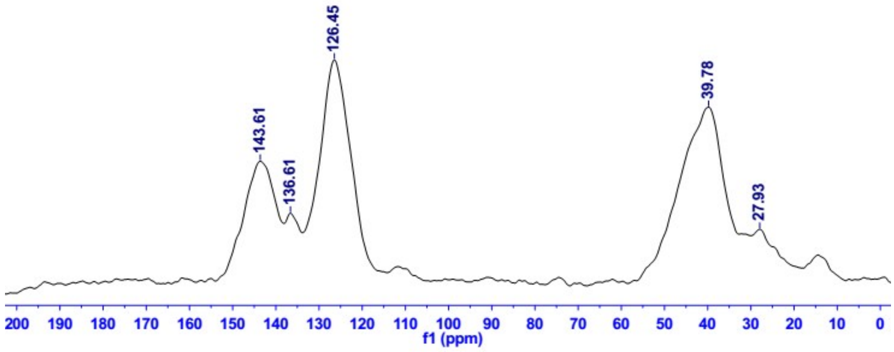

Fig. S16. Solid-state spectrum of Mg-Por\DVB(1:80)@POPs

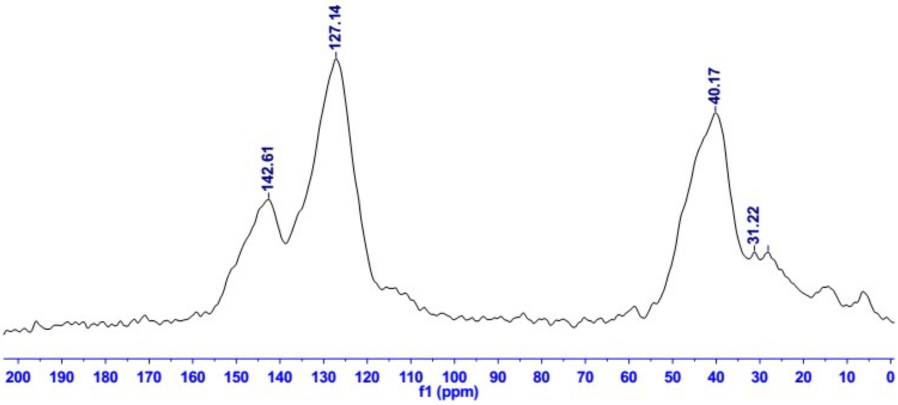

Fig. S17. Solid-state spectrum of Mg-Por\DVB(1:100)@POPs

Elemental analysis data

Table S3. Elemental analysis data of the five Mg-Por\DVB@POPs samples

Theoretical values			
Sample	**C wt%**	**H wt%**	**N wt%**
Mg-Por\DVB(1:20)@POPs	90.48	7.11	1.68
Mg-Por\DVB(1:40)@POPs	91.26	7.39	0.94
Mg-Por\DVB(1:60)@POPs	91.56	7.50	0.66
Mg-Por\DVB(1:80)@POPs	91.72	7.55	0.50
Mg-Por\DVB(1:100)@POPs	91.82	7.60	0.41
Experimental values			
Mg-Por\DVB(1:20)@POPs	90.50	7.08	1.65
Mg-Por\DVB(1:40)@POPs	91.29	7.37	0.92
Mg-Por\DVB(1:60)@POPs	91.60	7.52	0.63
Mg-Por\DVB(1:80)@POPs	91.75	7.58	0.49
Mg-Por\DVB(1:100)@POPs	91.85	7.64	0.39

Table S4. Comparison of elemental analysis data and ICP data of the five Mg-Por\DVB@POPs samples

Sample	Mg content calculated from elemental analysis (wt%)	Mg content tested from ICP analysis (wt%)
Mg-Por\DVB(1:20)@POPs	0.77	0.70
Mg-Por\DVB(1:40)@POPs	0.42	0.38
Mg-Por\DVB(1:60)@POPs	0.25	0.29
Mg-Por\DVB(1:80)@POPs	0.18	0.20
Mg-Por\DVB(1:100)@POPs	0.12	0.19

XPS analysis of Mg bonding energy of the five Mg-Por\DVB@POPs samples

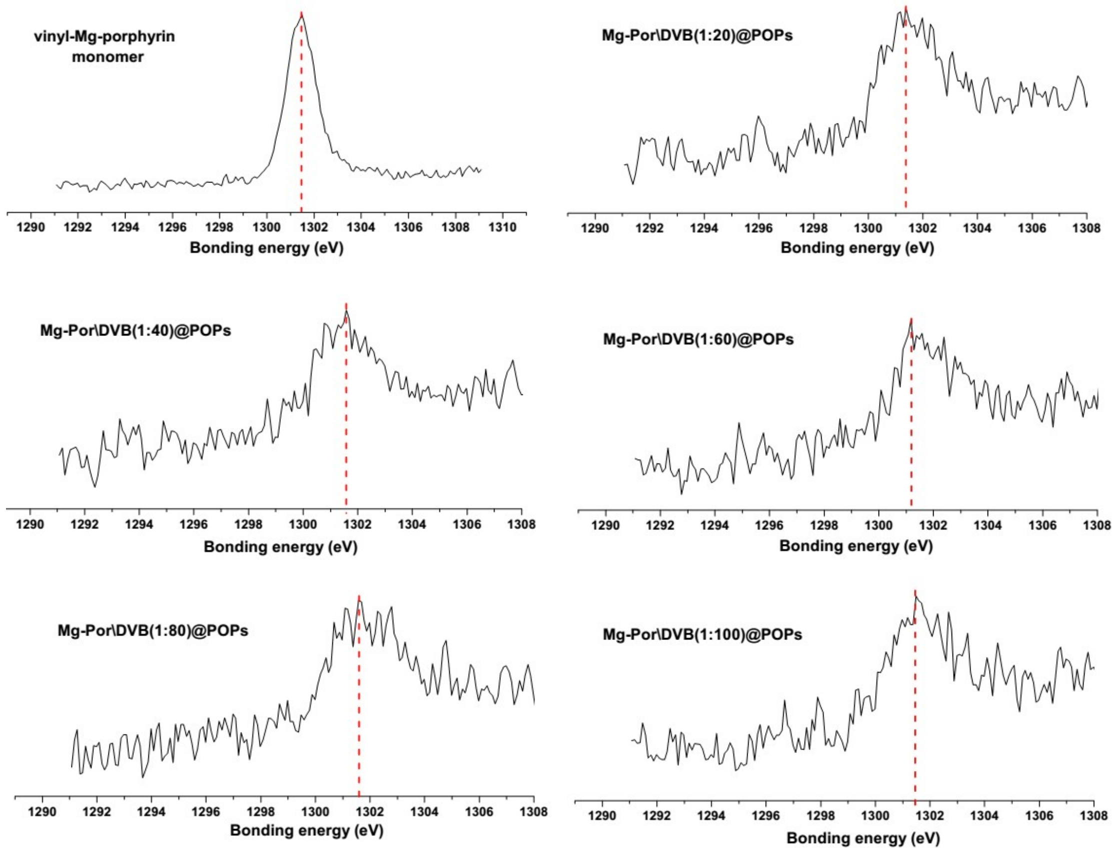

Fig. S18. XPS analysis of Mg bonding energy of the vinyl-Mg-porphyrin monomer and five Mg-Por\DVB@POPs samples